



EUROTHERM112-K108

## **Corrosion inhibitors for TES material at high temperature for CSP plants**

Angel G. Fernández\*, Luisa F. Cabeza

GREiA Research Group, INSPIRES Research Centre, Universitat de Lleida, Pere de Cabrera s/n, 25001-Lleida, Spain, e-mail: [angel.fernandez@diei.udl.cat](mailto:angel.fernandez@diei.udl.cat)

### **Abstract**

Molten salt technology using nitrate salts as thermal energy storage material is the current state-of-the-art of concentrated solar power technology and power tower central receivers are currently limited by the maximum operating temperature of their working fluid. The limit of solar salt (60wt.% NaNO<sub>3</sub> + 40wt.% KNO<sub>3</sub>) thermal stability is around 565°C with ambient air as the cover gas. In order to obtain higher efficiency goals using molten salt technologies working at higher temperatures (e.g., 650°C to 750°C), a different salt chemistry is required for new generation of CSP plants and chlorides molten salts could be a feasible option. Corrosion mitigation could solve the current issues related with the use of chloride salt at high temperature. In this work, the proposal of different corrosion mitigation strategies has been evaluated, as well as the identification of the most corrosive impurities present in the ternary chloride salt composed by MgCl<sub>2</sub>/KCl/NaCl (60/20/20 mol%). For this purpose, electrochemical impedance spectroscopy tests were carried out at 700°C on austenitic stainless steel (AISI 304) and a Ni base alloy (Inconel 702) during 100 hours. In this case, MgOHCl was identified as the main important corrosive impurity, present in the chloride salt, to control in the storage system. Regarding the materials tested, Ni base alloy (Inconel 702) showed the most promising results for their use as container material.

**Keywords:** Chloride molten salt; Thermal energy storage; Corrosion mitigation



## 1. Introduction

According International Energy Agency (IEA) [1], CSP is expected to grow 87% (4.3 GW) over the forecast period 2018-2023, 32% more than in 2012-17. China leads at 1.9 GW, followed by 1 GW from projects that receive multilateral development bank support in Morocco and South Africa, 1 GW in the Middle East, and 300 MW each in Australia and Chile.

Since Spain and the United States, the two countries with the most installed capacity, are not expected to commission projects over the forecast period, China is expected to overtake the United States to have the second-largest CSP capacity installed by 2023. Recent auction results indicate significant cost-reduction potential, but technology risk, restricted access to financing, long project lead-time, and market designs that do not value thermal energy storage continue to challenge CSP deployment [1].

An opportunity has been identified recently to obtain higher power generation efficiencies through integration of supercritical CO<sub>2</sub> (sCO<sub>2</sub>) Brayton power cycle. To achieve this integration, CSP needs to operate at temperatures above 550°C requiring advanced, high-temperature heat transfer fluids in the range of 550°C to 750°C. The selection of a high-temperature molten salt chemistry is needed, as well as the need to understand its impact on containment materials that can achieve acceptable strength, durability, and cost targets at these high temperatures [2].

Because of their low cost and high decomposition temperature, molten chlorides are considered good candidates. However, these molten salts introduce a set of technological and engineering challenges because of their very corrosiveness to typical containment materials. Corrosion mitigation approaches have been investigated to achieve a corrosion rate around 20 μm/yr or lower for the containment materials, thus providing a plant lifetime of 30 years or longer [3-6].

The aim of this paper is to analyse the different corrosion mitigation strategies present in the literature for chloride molten salts.

## 2. Corrosion mitigation strategies

Corrosion mitigation is one of the most important issues for the new generation of TES materials. Different corrosion protection methods are available in order to reduce the materials' corrosiveness and improve the operation life of CSP plants. The different corrosion mitigation strategies for molten chlorides are shown in Figure 1.

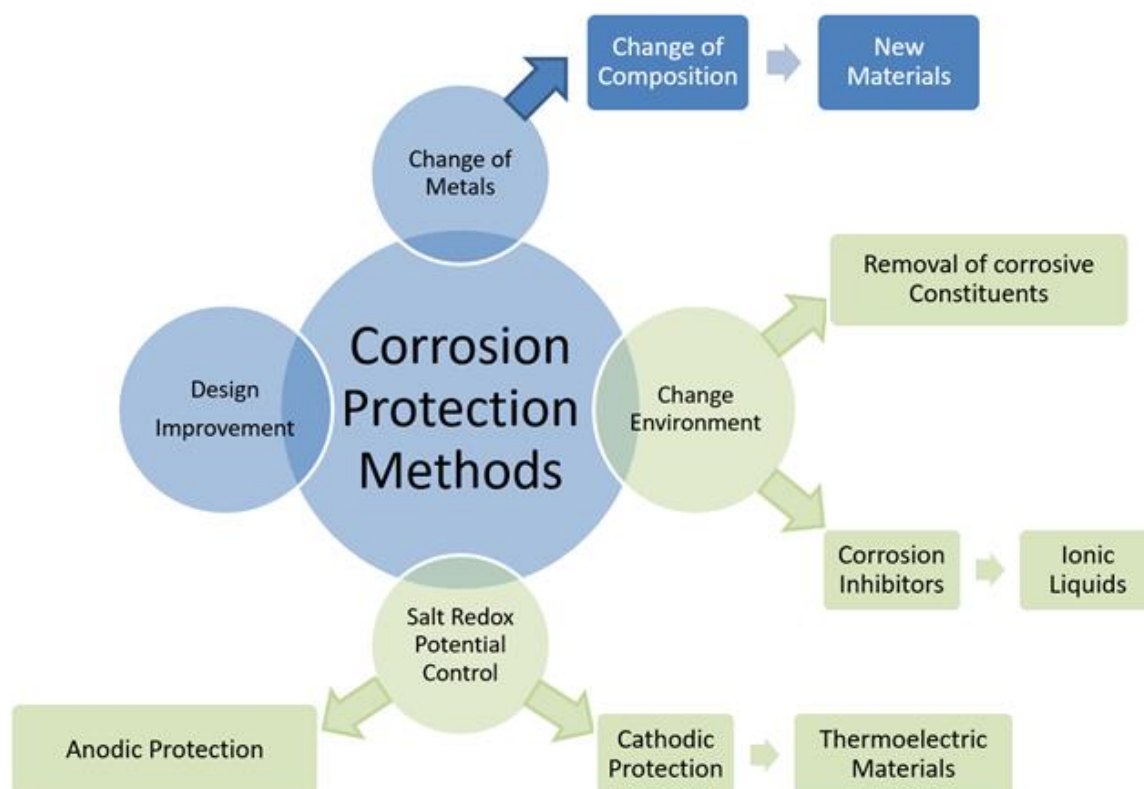


Figure 1. Corrosion protection methods applied to molten salt environments

Additionally to a proper system design and the selection of the more resistant alloys to be in contact with the corrosive environment, some of these corrosion mitigation possibilities have been performed in the literature.

Regarding chloride salts, Zn-based chlorides present the lowest melting point but they also have the lowest heat capacity and a measurable vapour pressure which disperses  $ZnCl_2(g)$  in the headspace that can cause salt deposition throughout the valves and joints [2]. Even though Mg-based chlorides have higher melting point than Zn-based ones, they are better because they have lower cost and higher heat capacity. Their corrosion can also be mitigated via melt redox potential control using active-metals such as Mg. However, they require no oxygen/water in the atmosphere [2] and addition of elemental Mg into the salt poses concerns regarding Mg-Ni intermetallic formation that melts at 512°C.

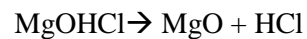
One of the key efforts in molten chloride corrosion mitigation has been focused on reducing the corrosive impurities by suppressing the side reactions of hydrolysis during salt heating [7-9]. One of the most studied mixtures is composed of  $\text{MgCl}_2\text{-NaCl-KCl}$  (60-20-20 mol%) since it has a melting point of  $380^\circ\text{C}$ , thermal stability up to  $800^\circ\text{C}$ , higher heat capacity compared to chloride salts containing  $\text{ZnCl}_2$ , and low vapour pressure. In this salt,  $\text{MgCl}_2$  is in the form of hexahydrate (i.e., 6 molecules of water) and  $\text{MgOHCl}$  has been detected as the most corrosive impurity which is formed through the following reaction at  $167^\circ\text{C}$  [10]:



The dehydration of the monohydrate occurs at  $235^\circ\text{C}$  which also produces  $\text{MgOHCl}$ :



Thermal decomposition of  $\text{MgOHCl}$  was reported to occur at  $415^\circ\text{C}$  [10] which produces  $\text{MgO}$  and  $\text{HCl}$ :



## 2.1 Corrosion inhibitors

The use of corrosion inhibitors (CIs) added to molten salt has been extended in the last years along with the use of  $\text{MgO}$ ,  $\text{CeO}_2$  and  $\text{DyO}_2$  to help reduce corrosion in the alloys [11]. Some researchers have highlighted a new way to mitigate corrosion by adding different redox couples to fix the salt's potential [12], which could be key to future developments since it implies the variation in the molten salt corrosive potential. Utilization of ionic liquids could be a new strategy since they can block the anodic and cathodic sites present on the metal surface in contact with molten chloride salts. What makes ionic liquids even more attractive is their properties such as lower melting point (lower than  $100^\circ\text{C}$ ), high polarity, low toxicity, low vapour pressure, high thermal and chemical stability, and less environmental hazard. Ionic liquids, also known as “designer chemicals”, can be engineered to have desired properties by proper selection of cations and anions, which is the greatest advantage of using ionic liquids [13].

## 2.2 Salt redox potential control

Two strategies are presented below.

### 2.2.1 Anodic protection

During the last years, the proposal of Alumina Forming Alloys (AFA) as storage container material has seen a significant increase due to their better corrosion resistant behaviour obtained by the formation of the alumina protective layers compared to chromia that is usually used in commercial stainless steel [14,15].

Gomez-Vidal [3] evaluated alumina-forming alloys (AFA) exposed to molten 35.59 wt%  $MgCl_2$  – 64.41 wt%  $KCl$  at 700°C in a flowing Ar atmosphere. In this research, alumina-forming alloys Inconel 702 (IN702), Haynes 224 (HR224), and Kanthal APMT (APMT) were pre-oxidized at different temperatures, for different dwelling times, and in different atmospheres to produce the protective, passivation oxides at the surface. Both electrochemical tests and conventional long-term test based on weight-change were used to down-select the best-performing alloy and surface pre-oxidation conditions. Because  $MgCl_2$  is highly hygroscopic, the authors performed a controlled drying/purification process to minimize the presence of corrosive oxygen-containing compounds in the molten salt.

Linear sweep voltammetry (LSV) measurement and sample characterization showed that the best-performing alloy was In702 pre-oxidized in zero air (ZA) at 1050°C for 4 h due to the presence of more stable alumina layers.

Ding et al. [16] studied the hot corrosion behaviour of three commercial alloys (310SS, In800H and hastelloyC270) in the eutectic  $MgCl_2/NaCl/KCl$  mixture at 700°C for 500 hours. Regarding the corrosion resistance, Hastelloy showed a better behaviour (79  $\mu m/year$ ) compared to Inconel (364  $\mu m/year$ ) and 310SS (1581  $\mu m/year$ ).

These authors [9] performed a comprehensive review of the corrosion test carried out in the literature using chloride molten salt. Results showed that, at temperatures up to 700°C, the corrosion rate obtained was higher than that needed to achieve the target lifetime of 30 years (20  $\mu m/year$ ). For this reason, the corrosion mitigation strategies proposed in this research are key to successful development of the next generation CSP plants.

### 2.2.2 Cathodic protection

Cathodic protection has been proposed in the literature to mitigate corrosion of super alloys in molten salts. At a high level, a sacrificial metal that more easily “corrodes” is to prevent corrosion of the super alloy or its components.

Since the corrosion reaction kinetics is so fast and the means to reduce mass transfer (without drastically change the metal or salt composition/properties) might not be readily available, a key strategy to mitigate corrosion is to inhibit corrosion at the thermodynamic level. The reduction potential of various metal elements in chlorides can be easily obtained from the chloride



Ellingham Diagram which tells which metal species is stable in a certain chloride salt. By adding Mg metal into the molten  $\text{MgCl}_2$ -KCl mixture where Mg solubility is sufficiently high [17], the reduction potential of the alloy components can be shifted by more than 0.5 V such that both  $\text{Cr}^{2+}$  and  $\text{Cr}^{3+}$  are less stable than the cations in the molten salt mixture. The most thermodynamically stable form of chromium is hence the metallic chromium in the alloy meaning oxidation of chromium will not occur.

Finally, a novel approach for cathodic protection can be introduced. It has been reported that solid salts, such as sodium chloride (NaCl) or zinc chloride ( $\text{ZnCl}_2$ ), are normally considered to be electrical insulators [18]; however, when the salts are melted, they become conductive and exhibit thermoelectric properties (although electrical transport in fused salts occurs by movement of ions rather than electrons). In particular, fused salts show large values of the Seebeck coefficient from 300 to 900 microvolts per °C [18]. Those values could be used for produce a cathodic protection over the storage tank steel, giving a suitable solution to control the corrosion risks in the new generation of CSP plants using molten chlorides.

### 3. Experimental Procedure

The molten salt tested was the eutectic mixture  $\text{MgCl}_2/\text{NaCl}/\text{KCl}$  (60/20/20 mol%, Sigma Aldrich 99%) at 700°C under inert atmosphere ( $\text{N}_2$ ). Electrochemical impedance tests were obtained in a frequency range between 100 kHz and 10 mHz. Linear polarization tests were carried out from a potential of -0.6 to 0.4 V of the OCP voltage. The scanning range is 0.005 V/s with steps of 0.00244 V.

Working electrode (WE) and reference-counter (RE-CE) electrodes were immersed in the molten salt (electrolyte) and the Open Circuit Potential (OCP) was measured using a potentiostat (Gamry 1010E) connected to the system through a Cr-Ni wire. The experimental set up is shown in Figure 2.

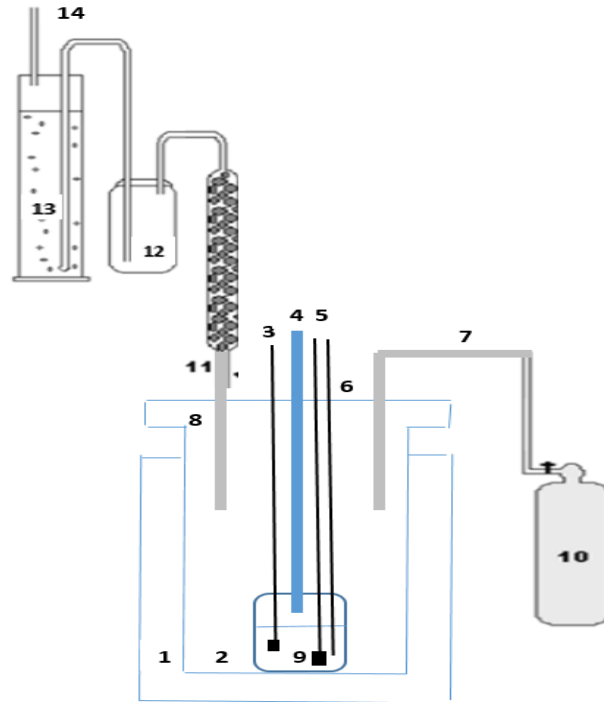


Figure 2. Experimental setup of electrochemical test in controlled atmosphere: 1: furnace; 2: molten salt reactor; 3: counter electrode, 4: thermocouple, 5: working electrode, 6: Reference electrode, 7: gas inlet, 9: molten salt, 10: carrier gas, 8: off-gas system (which consists of 11: MgO trap for chlorine; 12: moisture removal; 13: 1 M NaOH scrubber; and 14: gas exhaust.

In the preliminary tests carried out, the materials evaluated were a ferritic stainless steel (AISI 430) and a Ni base alloy (In702), with the chemical composition shown in Table 1.

Table 1. Chemical composition of material immersed in chloride molten salt

Material	Weight (%)					
	Al	Mn	Ni	Cr	Ti	Fe
<b>AISI430</b>	-	0.2	0.18	16.21	0.02	Balance
<b>In 702</b>	3.2	-	Balance	15.52	-	2

## 4. Results

Preliminary results for linear polarization tests in In702 and AISI 430 immersed during 100 h are shown in Figure 3.

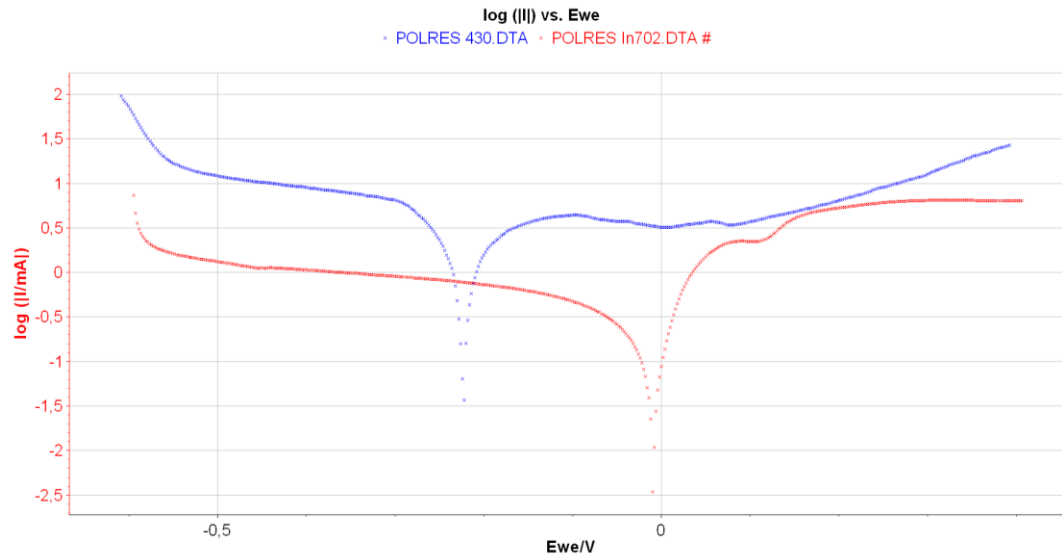


Figure 3. Linear polarization resistance results for In702 and AISI 430 immersed in chloride molten salts during 100 hours at 700°C.

Fitting the linear polarization graphs (Tafel curves), the corrosion rates obtained were 6.432 mm/year for AISI 430 and 1.062 mm/year for In702.

## 5. Conclusions

Corrosion mitigation strategies are key in order to control the corrosion potential in chloride molten salts. The main conclusions found were:

1. Alumina scales formed in AFA alloys present a higher corrosion protection in the material surface.
2. MgOHCl was identified as the most important corrosive impurity and a specific thermal treatment needs to be developed before corrosion tests.
3. Preliminary results showed a better corrosion resistance for Ni base alloys compare to stainless steel.





## Acknowledgements

The research leading to these results has received funding from Spanish government (ENE2015-64117-C5-1-R (MINECO/FEDER)). The authors would like to thank the Catalan Government for the quality accreditation given to their research group GREiA (2017 SGR 1537). GREiA is a certified agent TECNIO in the category of technology developers from the Government of Catalonia. Angel G. Fernández wants to acknowledge the financial support from the European Union's Horizon 2020 research and innovation programme under the Marie Skłodowska-Curie grant No 712949 (TECNIOspring PLUS) and from the Agency for Business Competitiveness of the Government of Catalonia. This work is partially supported by ICREA under the ICREA Academia programme.

## References

1. Agency, I.E., *Renewables 2018: Market analysis and forecast from 2018 to 2023* [www.iea.org](http://www.iea.org), 2018.
2. M. Mehos, C.T., J. Vidal, M. Wagner, Z. Ma, C. Ho, W. Kolb, C. Andracka and A. Kruiženga, *Concentrating Solar Power Gen3 Demonstration Roadmap*. Technical Report, NREL/TP-5500-67464, 2017.
3. J. Gomez-Vidal, A.G. Fernandez, R. Tirawat, C. Turchi, W. Huddleston, *Corrosion resistance of alumina-forming alloys against molten chlorides for energy production. I: Pre-oxidation treatment and isothermal corrosion tests*. Solar Energy Materials and Solar Cells.
4. J. Gomez-Vidal, A.G. Fernandez, R. Tirawat, C. Turchi, W. Huddleston, *Corrosion resistance of alumina forming alloys against molten chlorides for energy production. II: Electrochemical impedance spectroscopy under thermal cycling conditions*. Solar Energy Materials and Solar Cells.
5. Vignarooban, K., *Vapor pressure and corrosivity of ternary metal-chloride molten-salt based heat transfer fluids for use in concentrating solar power systems*. Applied Energy. 2015, 159: p. 206-213.
6. Kruiženga, A.M., *Corrosion Mechanisms in Chloride and Carbonate Salts*. Sandia Report, 2012. SAND2012-7594.
7. M. M. Avedesian and H. Baker, in ASM Specialty Handbook: Magnesium and Magnesium Alloys.
8. H. E. Friedrich and B. L. Mordike, *Magnesium Technology: Metallurgy, Design Data, Automotive Applications*, Springer ebook collection / Chemistry and Materials Science 2005–2008, Edition illustrated, Springer Science & Business Media., p.35, 2006.
9. Ding, W., A. Bonk, and T. Bauer, *Corrosion behavior of metallic alloys in molten chloride salts for thermal energy storage in concentrated solar power plants: A review*. Frontiers of Chemical Science and Engineering. 2018, 12: p. 564-576.
10. Q. Huang, G. Lu, J. Wang, J. Yu, Thermal decomposition mechanisms of  $MgCl_2 \cdot 6H_2O$  and  $MgCl_2 \cdot H_2O$ . Journal of Analytical and Applied Pyrolysis, 2011, 91, pag: 159-164
11. B. Xu, P. Li, Extending the validity of lumped capacitance method for large Biot number in thermal storage application. Solar Energy. 2014, 105: p. 71-81.
12. M. Gibilaro, L. Massot, and P. Chamelot, A way to limit the corrosion in the Molten Salt Reactor concept: the salt redox potential control. Electrochimica Acta. 2015, 160: p. 209-213.



13. A. M. Atta, G. A. El-Mahdy, H. A. Al-Lohedan, A. Rahman, O. Ezzat, A New Green Ionic Liquid-Based Corrosion Inhibitor for Steel in Acidic Environments. *Molecules* 2015, 20, Pag: 11131-11153
14. Brady, M.P., *Effects of minor alloy additions and oxidation temperature on protective alumina scale formation in creep-resistant austenitic stainless steels*. *Scripta Materialia*, 2007, 57: p. 1117-1120.
15. Brady, M.P., *Co-optimization of wrought alumina-forming austenitic stainless steel composition ranges for high-temperature creep and oxidation/corrosion resistance*. *Materials Science & Engineering A*, 2014. 590: p. 101-115.
16. Ding, W., et al., *Hot corrosion behavior of commercial alloys in thermal energy storage material of molten MgCl<sub>2</sub>/KCl/NaCl under inert atmosphere*. *Solar Energy Materials and Solar Cells*. 2018, 184: p. 22-30.
17. M. Krumpelt, J. Fischer, and I. Johnson, "The Reaction of Magnesium Metal with Magnesium Chloride," *J. Phys. Chem.*, vol. 72, no. 2, pp. 506–511, 1968.
18. Jacob Greenberg, Lawrence H. Thaller, Donald E. Weber. A possible regenerative, molten-salt, thermoelectric fuel cell. Nasa technical note TN D2440 (1964)